Article:
Elgayar, I, Hill, R, Chen, X et al. (2 more authors) (2017) Dielectric spectroscopy and dissolution studies of bioactive glasses. International Journal of Applied Glass Science, 8 (4). pp. 418-427. ISSN 2041-1286

https://doi.org/10.1111/ijag.12324

Dielectric Spectroscopy and Dissolution Studies of Bioactive Glasses

Iman Elgayar[a], Robert Hill[b], Xiaojing Chen[b], Nigel Bubb[c] and David Wood[c]

[a]Department of Materials, Imperial College, London SW7 2BP, United Kingdom.

[b]Dental Physical Sciences, Institute of Dentistry, Queen Mary University of London, Mile End Road, London E1 4NS, United Kingdom

[c]Biomaterials and Tissue Engineering Research Group, School of Dentistry, University of Leeds, Welcome Trust Brenner Building, St James' University Hospital, Leeds LS9 7TF, United Kingdom

Abstract

The first and rate-limiting step in the degradation of bioactive glasses is thought to be the ion exchange of hydrated protons in the external fluid with alkali metal cations in the glass. The activation energy (E_a) for alkali ion hopping can be followed by dielectric spectroscopy. The replacement of CaO by Na_2O resulted in a reduction in the E_a for ion hopping. In contrast, increasing the glass network connectivity or reducing the non-bridging oxygen content of the glass resulted in an increase in E_a. Substitution of K_2O for Na_2O had little influence on E_a. Mixing alkali metals increased the E_a as expected on the basis of the mixed alkali effect. There was no correlation between the E_a for ion hopping and the dissolution behaviour of the glass. Furthermore the activation energy for Si, Ca Na and K ion release was found to be approximately a factor of three lower than that for ion hopping suggesting that another rate controlling mechanism is important in the degradation of bioactive glasses. The presence of a second relaxation process speculated that bioactive glasses undergo amorphous phase separation into silica rich and orthophosphate rich phases and the two relaxation processes are due to ion hopping in the two phases.

Key words: bioactive glass, activation energy, degradation, mixed alkali, dielectric spectroscopy

Introduction

A bioactive glass undergoes degradation in physiological fluids [1]. The first step is believed to be the ion exchange between the sodium ions in the glass and the proton ions from the external solution. The diffusion of the sodium cations through the glass is thought to be a rate-limiting step. The second step is thought to be the base catalysed hydrolysis of Si-O-Si bonds of the glass structure [2]. Subsequent steps involve the formation of a silica-gel and the resulting formation of a hydroxycarbonated apatite layer on the surface leading to osseointegration and a bonded interface when a bioactive glass is implanted into bone. This mechanism is based on the previous corrosion studies of alkali silicate glasses, which are well documented, as well as infra-red spectroscopy studies which appear to show the formation of $Si\text{-}O^-$ species following Si-O-Si bond breakage [3, 4]. However the mechanism proposed, and particularly the first two steps, is not predictive of the reactivity of bioactive glasses as a function of their compositions.

A number of authors including Rawlings [5] Hill [6], Strnad [7] and more recently Brauer and Hill [8] have suggested that the degree of network connectivity may be an important aspect and can be used to predict the degradation rate and bioactivity of glasses. Hill has followed the approach of Ray [9] who viewed silicate glasses as inorganic polymers of oxygen crosslinked by silicon atoms. The properties of such glasses may be explained on

the basis of the crosslink density or network connectivity of the glass network using concepts taken from polymer science that are normally used to predict the behaviour of organic polymers. The network connectivity or crosslink density of a glass can be used to predict their surface reactivity, solubility, expansion coefficient and the likelihood of undergoing glass in glass phase separation. For example: the lower the crosslink density the lower the glass transition temperature [10, 11], and the greater the reactivity and solubility. In general the reactivity and solubility of inorganic glasses changes dramatically at the point where the glasses move from being continuous cross-linked networks to linear polymers of decreasing molar mass. The transition from a three dimensional network to a linear polymer occurs at zero crosslink density or a network connectivity of two. The network connectivity is defined as the average number of bridging oxygen bonds per silicon. A glass with a network connectivity of two is thought to correspond to a linear polymer chain or a ring structure, whilst a pure silica glass has a network connectivity of four. The network connectivity model can be used to predict the bioactivity of glasses to a certain degree [8]. It works best for simple SiO_2-CaO and SiO_2-CaO-Na_2O glasses, but does not work well for the phosphate containing compositions in clinical use.

Recently, Tiloca et al. [12, 13] have carried out molecular dynamics simulations of the structure of bioactive glass compositions. These simulations suggest that the bioactivity arises largely from the presence of a very fragmented glass network. However, unlike the MAS-NMR data more than two different Q species are present in these simulations. A study looking at the role of phosphate suggests that the phosphate will phase separate into phosphate rich domains at between 5 and 12mol % of P_2O_5 content. This phase separation is driven by the preferential association of Na^+ and Ca^{2+} cations with orthophosphate PO_4^{3-}

ions. This observation from MD studies is supported by the experimental ^{31}P MAS-NMR experiments[14]. Experimentally evidence is found for phosphorus forming orthophosphate at lower mole percentages of P_2O_5 than that found in the MD studies.

Despite the extensive studies of bioactive glasses were reported in the literature, there are relatively few systematic studies of compositions where alkali metals other than sodium have been investigated [14, 15]. Furthermore there is very few detailed study of mixed alkali glasses where both sodium and potassium have been incorporated into bioactive glasses [14], despite the fact that mixing alkali metal ions in glass is known to dramatically reduce the diffusion coefficient for alkali metal ion diffusion, decrease electrical conductivity, corrosion and dissolution rates, and increase the activation energy for ion hopping [16].

The present paper investigates the activation energy for ion hopping of sodium containing, potassium containing and mixed alkali containing glasses, as well as their dissolution rate in order to have a good insight into the mechanisms involved in dissolution of bioactive glasses.

2.0 Experimental

2.1 Glass Design

The glasses were designed on the following basis. All substitutions were done on a molar basis, rather than a weight basis. Series A consists of glasses in which CaO is substituted for Na_2O. Series B is a Na_2O containing series of fixed Na_2O content where CaO is substituted for SiO_2 and the glass network connectivity is increasing. Series C is based on Series B and substituted all Na_2O with K_2O. Series D is a range of mixed alkali glasses

with the same total mole fraction of alkali metal oxide as the glasses in series B and C (Table 1 [17]). A standard commercially available bioactive glass 45S5 disc sample (20mm diameter, 2mm thick) was used for dielectric spectroscopy was provided by University of Vigos, Spain. The theoretical network connectivity of the glasses was calculated as following equation [18]:

$$NC = \frac{4[SiO_2]-2[M_2^IO+M^{II}O]+6[P_2O_5]}{SiO_2} \quad (1)$$

where M_2^IO and $M^{II}O$ present the mono and divalent modifier oxides, respectively in the glasses.

2.2. Sample preparation

According to the glass compositions (Table 1), each glass was prepared from Analar grade reagents $CaCO_3$, Na_2CO_3, K_2CO_3, P_2O_5 and SiO_2. Reagents were melted in platinum crucibles at the melting temperatures for 1hr. The melts were rapidly quenched into water to prevent phase separation. The glass frit was ground in a Gyro Mill for 14 mins and sieved for 30 mins in a mechanical shaker to obtain <45 µm particles.

Glass rods of 10 mm diameter for each composition were cast as described by Elgayar et al.[17]. The obtained glass rods were then sectioned into 10 mm diameter by approximately 1 mm thick discs for dielectric spectroscopy. The samples were polished using a 1200 grit silicon carbide paper prior to dielectric analysis.

2.3 Dielectric Spectroscopy

A Polymer Laboratories Dielectric Thermal Analyser, DETA (Polymer Laboratories, Epinal Way, Loughborough UK) was used for obtaining the real part of the dielectric constant (ε') and the dielectric loss factor (tan δ). Frequencies of 0.1, 1, 10, 25, 50 and 100

kHz were used with a heating rate of 2 °C/min over a temperature range from 30 to 500 ˚C. The activation for ion hopping was calculated from [19]:

$$f = A\frac{-E_{a(ih)}}{RT} \quad (2)$$

Where: A is the pre-exponential factor, f is the frequency in Hz, T is the maximum temperature in K, $E_{a(ih)}$ is the activation energy for ion hopping and R is the gas constant.

2.4 Dissolution Studies

Dissolution studies were carried out on all glass compositions. 0.075g of powder (<45μm) was immersed in 50ml of Tris-buffer (pH=7.25) [18] and placed in an orbital shaker at 1Hz, for time periods 5, 15, 30, 60, 120, 240 and 480 mins. Tris-buffer was used for these studies rather than the more conventional simulated body fluid (SBF), since the high concentration of sodium and calcium in SBF makes it difficult to determine the calcium and sodium ions released from the glasses. The concentrations of silicon, calcium, soduim and potassium ion were analyzed by inductively coupled plasma-optical emission spectroscopy (ICP-OES).

Dissolution studies were carried out at 20, 37 and 50 ^{o}C to study the activation energy of ion release, on three of the glass compositions ICIE9 (series A glass), ICIE14 (series B glass), and ICIE19 (series D glass). These glass compositions all have a network connectivity of 2.74. The same glass concentrations and settings were used as described above, however the dissolution was concentrated on shorter time periods: 1 min, 2 mins, 5 mins, 10 mins, 15 mins, 30 mins, 1 hr and 2 hrs.

3.0 Results and Discussion

Figure 1 shows the real part of the dielectric constant (ε') and the dielectric loss factor (tanδ) for the ICIE1 glass with the highest sodium content. Two distinct changes in ε' and two peaks in tanδ were observed for each frequency. This suggests that there are two distinct mechanisms of sodium ion hopping in this glass composition.

Solid state ^{31}P magic angle spinning nuclear magnetic resonance spectroscopy (MAS-NMR) of this glass [17] and all the other glasses studied in this paper indicate that the phosphorus is present largely as an orthophosphate type species and the phosphorus is not a part of the silicate glass network. ^{31}P MAS-NMR studies by O'Donnell et al. [14] also showed a clear evidence of orthophosphate species in soda line phosphosilicate glasses, whilst recently Pedone et al. [20] have shown the presence of orthophosphate and the absence of Si-O-P bonds in the 45S5 composition.

Since MAS-NMR probes the local environment around a nucleus and gives no information with regard to long-range order, it is not possible to determine whether there are orthophosphate clusters in the studied glasses or whether the glasses are phase separated into a silicate rich phase and a phosphate rich phase. However, the presence of two tan δ peaks from the dielectric data suggests that there are two sodium ion hopping mechanisms and this would indicate the hopping of sodium ions in two different phases. A phase is defined as a part of a material with structure and properties different from another. It is logical to conclude that one relaxation peak arises from hopping of sodium ions in the silicate rich phase and the other one in the orthophosphate rich phase. The other logical explanation is that the glass has undergone a very significant corrosion at the surface and the two sodium ion hopping mechanisms correspond to hopping in the bulk glass and in

the reacted surface. Nevertheless, this latter mechanism is thought to be unlikely, since great care was taken during samples preparation to avoid exposing them to water. Furthermore the incorporation of phosphate species into silicate glasses is widely known to induce amorphous phase separation [21] and the phase separation was found in bioactive glasses at a P_2O_5 content higher than 5 mol%, is supported by the MD studies [22]. It is interesting to know that in the MD simulation studies, fast cooling rate tends to suppress phase separation. However, casting glass into a rod sample takes longer time. Therefore, a phase separation might happen in the composition with a lower P_2O_5 content.

The activation energy for ion hopping for the two sets of relaxations for ICIE1 glass was calculated by plotting the natural log of the frequency against the reciprocal of the maximum of the tan δ peak in Kelvin (Figure 2). The activation energy for the lower temperature and higher temperature transitions are 76 and 87 kJ/mol, respectively. The activation energies for both transitions are very similar. Therefore, at this stage it is impossible to comment which transition corresponds to which phase.

Figure 3 shows the tan δ as a function of temperature for the second highest sodium content glass, ICIE2. The transitions have shifted up in temperature, as expected. This is due to the increase of the distance between non-bridging oxygen and sodium ion sites with a decrease in the sodium content, making the hopping process more difficult. At high frequencies the second relaxation process starts to approach the glass transition temperature and the upper operating temperature of the instrument and therefore, it is consequently obscured.

Figure 4 shows the tan δ for the lowest sodium content glass. Here only one set of the start of relaxation processes were evident due to the measuring limitation of the instrument and it was assumed that the second set of relaxation processes are above 500°C.

The activation energies for ion hopping calculated for all the A series of glasses where Na_2O is progressively substituted by CaO are shown in Figure 5. The activation energy increases from 76 to 160 kJ/mol with a decrease in Na_2O content from 26.38 to 6.6 mol%. The activation energies of the second set of relaxations for the two highest sodium content glasses are again comparable to that for the first set of relaxations.

Figure 6 shows the tan δ values as a function of temperature for the 45S5 composition. This glass is similar to the ICIE1 glass but has a slightly higher P_2O_5 content. Similar to ICIE1 glass, there are two sets of dielectric relaxations corresponding to two hopping mechanisms. The calculated activation energies are 79 and 82 kJ/mol. The activation energies for ion hopping of 45S5 were also shown in Figure 5 for a comparison purpose. As can be seen, its activation energies demonstrated good agreements with the ones for the A series of glasses.

The ^{31}P chemical shift of the orthophosphate from the MAS-NMR data is very sensitive to the charge balancing cations (Ca^{2+} and Na^{+}). The ^{31}P chemical shift of the glasses studied here [17, 23] and the 45S5 composition [24] correlates with the Na/Ca ratio of the original glass composition indicating that there is no preferential partitioning of sodium relative to calcium in either of the two phases. This may in part explain why there is little difference in the activation energies for ion hopping in the two phases of each glass.

All the glasses from Series B (sodium series of varying network connectivity), Series C (potassium series of varying network connectivity) and Series D (mixed alkali series of varying network connectivity) all showed one series of relaxation processes. The higher temperature set of relaxation processes presumably are higher than the operating

temperature of the instrument. The obtained activation energies for these glasses are exhibited in Figure 7. With the exception of the two potassium containing glasses with the lowest network connectivity, which showed significantly lower activation energies, the activation energy generally decreases slightly with increasing network connectivity for all three glass series. It might be thought that reducing the number of non-bridging oxygens in the glass would hinder the ion hopping process and increase the activation energy. However if it is assumed that the non-bridging oxygens linked to Ca^{2+} ions plays no role in the hopping of alkali metal cations, thus it will be the distance between non-bridging oxygens-Na/K^{+} pairs, which is important. Furthermore, incorporating CaO in the glass reduces the oxygen density, as shown inFigure 8. The oxygen density for the mixed alkali glasses series located between the Na series and the K glass series. The reduced oxygen density is thought to expand the glass network [25] and therefore increase the average distance between non-bridging oxygen-Na/K^{+} species thereby increasing the activation energy for ion hopping.

The activation energies for ion hopping of the single alkali sodium and potassium glasses with higher network connectivity (>2.4) are very similar to each other, while the activation energy for ion hopping of the mixed alkali sodium/potassium glasses is significantly higher than that for the single alkali containing glasses (Figure 7). This is expected on the basis of the well-known mixed alkali effect [16].

Whilst a detailed analysis of the dissolution kinetics was undertaken, for the purposes of brevity only a brief analysis specific to the dielectric results were presented here. Figure 9 shows the sodium release data for the A series glasses. The amount of sodium released increases with increasing Na_2O content of the glass, which is as expected and confirms a

previous study [26]. The calcium and silica release also increased with increasing Na_2O content. Figure 10and Figure 11 show the sodium and potassium released from the B, C and D series of glasses. The release decreases with increasing network connectivity of the glass. For example the amount of sodium released follows the order ICIE6 (NC=1.96) > ICIE3 (NC=2.04) > ICIE7 (NC=2.29) > ICIE8 (NC=2.47) > ICIE9 (NC=2.74). An identical correlation between the amount of potassium released and the network connectivity of the glass is found for the series C glasses. The sodium and potassium release of the mixed alkali glasses series D also correlates with the network connectivity. The release of sodium from series B is significantly higher than the release of potassium from series C. Previous studies [16, 27] have attributed the lower release of potassium relative to sodium to be due to the larger size of the K^+ cation. It is important to note that there is no significant difference in the mixed alkali metal release kinetics compared to the equivalent single alkali glasses. The mixed alkali glasses release very slightly more sodium (relative to the sodium content of the glass) than the single sodium glasses, whilst the reverse occurs for potassium. There is thus no evidence to suggest that mixing alkali metals in these glasses is inhibiting the corrosion/dissolution process. Whilst only the release of alkali metals is shown here, the calcium release and silicon release mirrored the alkali metal release data and followed the same trends.

There is little change in the dissolution behaviour of the glasses on substituting sodium for potassium or on mixing alkali. It is thought that the phosphate rich phase if present will not contribute significantly to the dissolution data, since the phosphate is likely to be the dispersed phase and is also present at low concentrations.

Surprisingly, there is no evidence of a mixed alkali effect reducing the corrosion rate despite the fact that the activation energy for ion hopping has increased significantly for the mixed alkali glasses compared to the single alkali glasses. The corrosion rate of the glasses falls markedly with increasing network connectivity despite a significant decrease in the activation energy for alkali metal ion hopping as the network connectivity is increased. Das and Douglas [28] reviewed the influence of temperature on the dissolution/degradation of silicate glasses by water, steam, dilute acids and dilute alkalis and found that nearly all the data fitted: $S = \exp\left[\frac{-E_{a(ir)}}{RT}\right]$ (3)

Where S is the corrosion rate, $E_{a(ir)}$ is the activation energy for ion release, R is the gas constant and T is the temperature. The activation energies obtained ranged between 60 and 100 kJ/mol and the activation energies correlated with those for alkali metal ion diffusion or ion hopping. The activation energy for dissolution was calculated for the ICIE9 a single alkali sodium glass, ICIE14 single alkali potassium glass and ICIE19 mixed alkali glass all with the same network connectivity of 2.74. All three glasses at all three temperatures gave linear plots of the concentration of released species against the square root of time. A typical plot is shown Figure 12. The slopes of these lines were then taken to get a rate of reaction/dissolution.

13 shows a typical plot of the log of the rate of dissolution against reciprocal temperature. Similar plots were obtained for the other glasses. Table 2 summaries the activation energies obtained for the different dissolving species for the three different glasses.

The activation energies for Si, Ca, Na and K release are all very similar and are fairly independent of whether the glass contains Na, K or contains mixed alkalis. The activation

energy is in the range 15-27 kJ/mol which is considerably lower than that obtained for ion hopping obtained by dielectric spectroscopy which is in the range 79-160 kJ/mol.

Arcos et al. [29] measured the activation of dissolution of a range of bioactive glasses most of which were sol-gel derived bioactive glasses, but included the 45S5 composition in their study and obtained an activation energy of about 9 kJ/mol for Si release into Tris buffer. This value is about halve of that obtained here, however it is worth pointing out that the 45S5 glass has a considerably lower NC (1.90) than the three glasses in which the activation energies were obtained here (NC=2.74). The higher NC values would be expected to reduce the degradation/dissolution rate and increase the activation energy for dissolution rate. Fagerlund and coworkers [30, 31] have recently measured the apparent activation energies to determine the dissolution control mechanisms based on hydrochloric acid consumption for the 45S5 glass composition and obtained values of 21 kJ/mol. They have also measured the activation from dissolution of Na (13-26 kJ/mol) and Ca (11-27 kJ/mol) in contrast to the values for the inert float glass and E-glass were higher and especially much higher for Si. These were in a good agreement with the data here and pointed to the mechanism of bioactive glass dissolution being fundamentally different from glasses of higher connectivity. It is also important to note that in Fagerlund et al.'s [31] elegant real time dissolution data in Tris buffer there is no preferential early release of some ions relative to others, but there appears to be almost congruent dissolution of the glass at early times.

It is widely assumed that the rate controlling step in the degradation rate of bioactive glasses is the ion exchange of protons for alkali metal cations. Given the larger size of Na^+ and K^+ cations relative to H^+ it would be expected that the diffusion of alkali metal cations and their activation energy for ion hopping would control the degradation process.

However there is relatively little correlation between the activation energy for ion hopping and that for dissolution/corrosion behaviour of the glasses. Series A glasses where CaO is substituted for Na_2O is the only series in which the activation energy for ion hopping increases and the glass dissolution or corrosion rate decreases. In series B, C and D where the network connectivity increases and the activation energy falls and the glass degradation or corrosion rate decreases. Furthermore the mixed alkali glasses have significantly higher activation energies for ion hopping, yet have dissolution rates almost identical to their single alkali counterparts. Mixing alkali metal ions has been frequently used as a method of reducing glass corrosion in silicate glasses; however, in these highly disrupted bioactive glasses it has no effect. The activation energies for dissolution are much lower than those for ion hopping. This contrasts with the data for the glasses with much higher network connectivity [32]. Douglas and Isard [32] found there was a strong correlation between the rate of removal of alkali metal ions and electrical conductivity, however subsequently Das and Douglas [28] showed that the correlation does not exist for less durable glasses of lower network connectivity and that the rate of extraction of alkali ions corresponds to diffusion coefficients 10^4-10^5 x greater than that obtained by electrical conductivity measurements. It is important to note here that the three glasses in which the activation energies for dissolution were determined were the three glasses of highest network connectivity. These glasses would be the ones that most likely to exhibit a correlation between the activation energy for ion hopping and the activation energy for dissolution/corrosion. Most corrosion studies of glasses have been centered on commercial soda lime silica compositions, which have NC of about 3 to 3.5. The results presented here suggest that alkali metal ion diffusion in the glass is not the rate-controlling step in

bioactive glasses degradation and that bioactive glasses may be distinctly different from the conventional much more durable silicate glasses of much higher network connectivity, thus, other mechanisms of degradation may be important. The fact that the rate controlling step does not correspond to alkali ion diffusion or hopping explains the complete absence of any mixed alkali effect on the corrosion dissolution behaviour of these glasses. This suggests that the disruption of the silicate glass network and the network connectivity are critical in determining bioactivity as proposed by Hill [6] Brauer and Hill [8], by the MD simulations by Tiloca et al. [12, 13] and more recently by Eden [33].

Conclusions

Dielectric spectroscopy shows that bioactive glasses exhibit two relaxation processes and the most likely explanation for this is that these glasses have undergone amorphous phase separation into a silicate rich phase and a phosphate rich phase. The activation energy for ion hopping decreases as CaO is substituted by Na_2O and decreases with increasing glass network connectivity. Na_2O and K_2O glasses generally have similar activation energies for ion hopping whilst the mixed alkali glasses have much higher activation energies for ion hopping than the comparable single alkali glasses. There is no correlation between the activation energy for ion hopping and either the rate of dissolution of the glass or the activation energy for dissolution/corrosion suggesting that alkali metal ion diffusion is not the rate limiting step in glass dissolution. This conclusion is supported by the absence of a mixed alkali effect in the dissolution/corrosion behaviour. The mechanism of corrosion/dissolution is therefore fundamentally different to that of more durable silicate

glasses and the fragmented silicate structures in the glass are critical in determining the bioactivity of silicate glasses.

The phase separation to a phosphate rich phase and silicate rich phase is consistent with Eden's split network model [33] and has significant implications for the dissolution of bioactive glasses. For example the orthophosphate rich phase is likely to be very soluble and this phase when exposed on the surface of bioactive glasses is likely to dissolve much more rapidly than the silicate phase. This latter point has been also emphasized by Tilocca et al. [13, 22] in their recent MD simulation of phosphosilicate glasses.

Acknowledgements

The authors would like to thank the EPSRC for a scholarship for Iman Elgayar and Professor Rees Rawlings (Imperial College), Dr. Alistair McCormack (Alfred University), Dr. Antonio Tilocca (University College London) and Professor Malcom Ingram (University of Aberdeen) for the useful comments and discussions on the manuscript prior to submission.

References

[1] L.L. Hench, J. Wilson, An introduction to bioceramics, World scientific1993.
[2] L.L. Hench, Bioceramics-from concept to clinic, Journal of the American Ceramic Society 74(7) (1991) 1487-1510.
[3] O. Andersson, G. LaTorre, L. Hench, The kinetics of bioactive ceramics. Part II. Surface reactions of three bioactive glasses, Bioceramics: 3rd Intl Symp Ceramics in Medicine, 1992.
[4] M.R. Filgueiras, G. La Torre, L.L. Hench, Solution effects on the surface reactions of a bioactive glass, Journal of Biomedical Materials Research Part A 27(4) (1993) 445-453.
[5] R. Rawlings, Composition dependence of the bioactivity of glasses, Journal of materials science letters 11(20) (1992) 1340-1343.
[6] R. Hill, An alternative view of the degradation of bioglass, Journal of Materials Science Letters 15(13) (1996) 1122-1125.
[7] Z. Strnad, Role of the glass phase in bioactive glass-ceramics, Biomaterials 13(5) (1992) 317-321.
[8] R.G. Hill, D.S. Brauer, Predicting the bioactivity of glasses using the network connectivity or split network models, Journal of Non-Crystalline Solids 357(24) (2011) 3884-3887.
[9] N.H. Ray, Inorganic polymers, Academic Press1978.
[10] M.D. O'Donnell, Predicting bioactive glass properties from the molecular chemical composition: Glass transition temperature, Acta Biomaterialia 7(5) (2011) 2264-2269.
[11] R.G. Hill, D.S. Brauer, Predicting the glass transition temperature of bioactive glasses from their molecular chemical composition, Acta Biomater 7(10) (2011) 3601-5.
[12] A. Tilocca, A.N. Cormack, N.H. de Leeuw, The formation of nanoscale structures in soluble phosphosilicate glasses for biomedical applications: MD simulations, Faraday discussions 136 (2007) 45-55.
[13] A. Tilocca, A.N. Cormack, Structural effects of phosphorus inclusion in bioactive silicate glasses, Journal of Physical Chemistry B 111(51) (2007) 14256-14264.
[14] M.D. O'Donnell, S.J. Watts, R.V. Law, R.G. Hill, Effect of P2O5 content in two series of soda lime phosphosilicate glasses on structure and properties – Part II: Physical properties, Journal of Non-Crystalline Solids 354(30) (2008) 3561-3566.
[15] K. Wallace, R. Hill, J. Pembroke, C. Brown, P. Hatton, Influence of sodium oxide content on bioactive glass properties, Journal of Materials Science: Materials in Medicine 10(12) (1999) 697-701.
[16] D.E. Day, Mixed alkali glasses—their properties and uses, Journal of Non-Crystalline Solids 21(3) (1976) 343-372.
[17] I. Elgayar, A.E. Aliev, A.R. Boccaccini, R.G. Hill, Structural analysis of bioactive glasses, Journal of Non-Crystalline Solids 351(2) (2005) 173-183.
[18] A.L.B. Maçon, T.B. Kim, E.M. Valliant, K. Goetschius, R.K. Brow, D.E. Day, A. Hoppe, A.R. Boccaccini, I.Y. Kim, C. Ohtsuki, T. Kokubo, A. Osaka, M. Vallet-Regí, D. Arcos, L. Fraile, A.J. Salinas, A.V. Teixeira, Y. Vueva, R.M. Almeida, M. Miola, C. Vitale-Brovarone, E. Verné, W. Höland, J.R. Jones, A unified in vitro evaluation for apatite-forming ability of bioactive glasses and their variants, Journal of Materials Science: Materials in Medicine 26(2) (2015) 115.

[19] A. Jonscher, The Universal Dielectric Response: A Review of Data and Their Interpretation, Chelsea Dielectrics Group, University of London1979.
[20] A. Pedone, T. Charpentier, G. Malavasi, M.C. Menziani, New Insights into the Atomic Structure of 45S5 Bioglass by Means of Solid-State NMR Spectroscopy and Accurate First-Principles Simulations, Chemistry of Materials 22(19) (2010) 5644-5652.
[21] P.W. McMillan, "Glass Ceramic " second edition, Academic Press New York, 1979.
[22] A. Tilocca, Structure and dynamics of bioactive phosphosilicate glasses and melts from ab initio molecular dynamics simulations, Physical Review B 76(22) (2007).
[23] D.S. Brauer, N. Karpukhina, R.V. Law, R.G. Hill, Structure of fluoride-containing bioactive glasses, J. Mater. Chem. 19(31) (2009) 5629-5636.
[24] M.W.G. Lockyer, D. Holland, R. Dupree, NMR investigation of the structure of some bioactive and related glasses, Journal of Non-Crystalline Solids 188(3) (1995) 207-219.
[25] H. Doweidar, Density-structure correlations in silicate glasses, Journal of non-crystalline solids 249(2) (1999) 194-200.
[26] K.E. Wallace, R.G. Hill, J.T. Pembroke, C.J. Brown, P.V. Hatton, Influence of sodium oxide content on bioactive glass properties, Journal of Materials Science: Materials in Medicine 10(12) (1999) 697-701.
[27] M. Brink, T. Turunen, R.P. Happonen, A. Yli-Urpo, Compositional dependence of bioactivity of glasses in the system Na2O-K2O-MgO-CaO-B2O3-P2O5-SiO2, J Biomed Mater Res 37(1) (1997) 114-21.
[28] C. Das, R. Douglas, Studies on the reaction between water and glass. Part 3, Physics and chemistry of glasses 8(5) (1967) 178-184.
[29] D. Arcos, D. Greenspan, M. Vallet‐Regí, A new quantitative method to evaluate the in vitro bioactivity of melt and sol‐gel‐derived silicate glasses, Journal of Biomedical Materials Research Part A 65(3) (2003) 344-351.
[30] S. Fagerlund, Understanding the in vitro dissolution rate of glasses with respect to future clinical applications, (2012).
[31] S. Fagerlund, L. Hupa, M. Hupa, Dissolution patterns of biocompatible glasses in 2-amino-2-hydroxymethyl-propane-1, 3-diol (Tris) buffer, Acta biomaterialia 9(2) (2013) 5400-5410.
[32] R. Douglas, J. Isard, The action of water and of sulphur dioxide on glass surfaces, J. Soc. Glass Technol 33(154) (1949) 289-335.
[33] M. Edén, The split network analysis for exploring composition–structure correlations in multi-component glasses: I. Rationalizing bioactivity-composition trends of bioglasses, Journal of Non-Crystalline Solids 357(6) (2011) 1595-1602.

Figure 1. The dielectric constant (ε') and the dielectric loss factor (tan δ) as a function of temperature for the highest soda content glass (ICIE1) at different frequencies (the frequency increases from 0.1 to 100 Hz with the arrow pointing in direction.

Figure 2. The natural logarithm of frequency against the reciprocal of the maximum of the tan δ peak in Kelvin for glass ICIE1 (the highest Na2O content glass).

Figure 3. The tan δ plotted as a function of temperature for the glass ICIE2.

Figure 4. The tan δ plotted as a function of temperature for the lowest soda content glass ICIE4.

Figure 5. Activation Energy Plotted against Na_2O content for the A series glasses and the 45S5 composition, 5% error was applied. (□ = Relaxation 1 and ♦ = Relaxation 2)

Figure 6. The tan δ plotted against temperature for 45S5 glass.

Figure 7. Activation energies for ion hopping plotted against network connectivity, 5% error was applied. (▲= mixed alkali glasses; □= Na containing glasses; ♦= K containing glasses)

Figure 8. The influence of CaO content on the glass oxygen density. (▲= mixed alkali glasses; □= Na containing glasses; ♦= K containing glasses)

Figure 9. Sodium release as a function of time for the A series glasses. Y units corrected for relative molecular mass and normalized to Na content of glass.

Figure 10. Sodium release as a function of time for series B and D glasses. The numbers on the right represent the values of network connectivity. (▲= mixed alkali glasses and □= Na containing glasses)

Figure 11. Potassium release as a function of time for series C and D glasses. The numbers on the right represent the values of network connectivity. (▲= mixed alkali glasses and ♦= K containing glasses)

Figure 12. Calcium release for the ICIE9 glass plotted against the square root of time at ◆=20 ºC; ■=37 ºC and ▲=50ºC.

Figure 13. The log of the rate of dissolution against reciprocal temperature of ICIE9 for Ca release.

Table 1. Glass compositions (mol%), with their network connectivites (NC) and melting temperatures used.

	Glass	SiO_2	P_2O_5	CaO	Na_2O	K_2O	NC	Melt temp (^oC)
Series A	ICIE1	49.46	1.07	23.08	26.38	--	2.04	1370
	ICIE2	49.46	1.07	29.64	19.79	--	2.04	1420
	ICIE3	49.46	1.07	36.27	13.19	--	2.04	1450
	ICIE4	49.46	1.07	42.87	6.6	--	2.04	1475
	ICIE5	49.46	1.07	49.46	0.0	--	2.04	1500
Series B	ICIE6	48.46	1.07	37.27	13.19	--	1.96	1370
	ICIE3	49.46	1.07	36.27	13.19	--	2.04	1450
	ICIE7	53.46	1.07	33.27	13.19	--	2.29	1450
	IC IE8	56.46	1.07	30.27	13.19	--	2.47	1475
	ICIE9	61.00	1.07	25.27	13.19	--	2.74	1400
Series C	ICIE10	48.46	1.07	37.27	--	13.19	1.96	1370
	ICIE11	49.46	1.07	36.27	--	13.19	2.04	1420
	ICIE12	53.46	1.07	33.27	--	13.19	2.29	1450
	ICIE13	56.46	1.07	30.27	--	13.19	2.47	1475
	ICIE14	61.00	1.07	25.27	--	13.19	2.74	1400
Series D	ICIE15	48.46	1.07	37.27	6.60	6.60	1.96	1370
	ICIE16	49.46	1.07	36.27	6.60	6.60	2.04	1420
	ICIE17	53.46	1.07	33.27	6.60	6.60	2.29	1450

	ICIE18	56.46	1.07	30.27	6.60	6.60	2.47	1475
	ICIE19	61.00	1.07	25.27	6.60	6.60	2.74	1400
45S5	45S5	46.0	3.00	27.00	24.00	-	-	-

Table 2. Activation Energies (kJ/mol) for Si, Ca, Na and K ions release

Glass	**Ca ion release**		**Na ion release**		**K ion release**		**Si ion release**	
	$E_{a(ir)}$	**R^2**	**$E_{a(ir)}$**	**R^2**	**$E_{a(ir)}$**	**R^2**	**$E_{a(ir)}$**	**R^2**
ICIE9	19	0.82	19	0.99	--	--	27	0.75
ICIE14	17	0.94	--	--	17	0.85	20	0.91
ICIE19	16	0.96	24	0.86	15	0.79	22	0.99

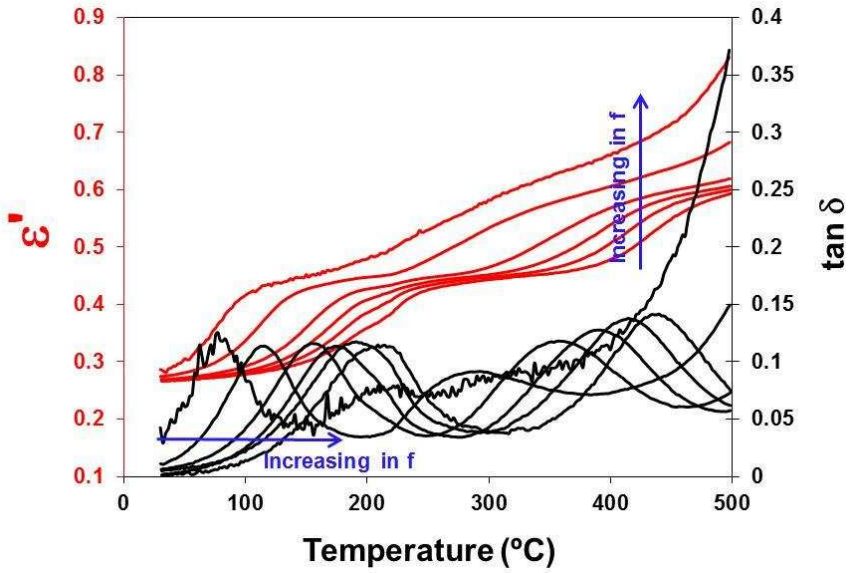

Figure 1. The dielectric constant (□') and the dielectric loss factor (tan □) as a function of temperature for the highest soda content glass (ICIE1).

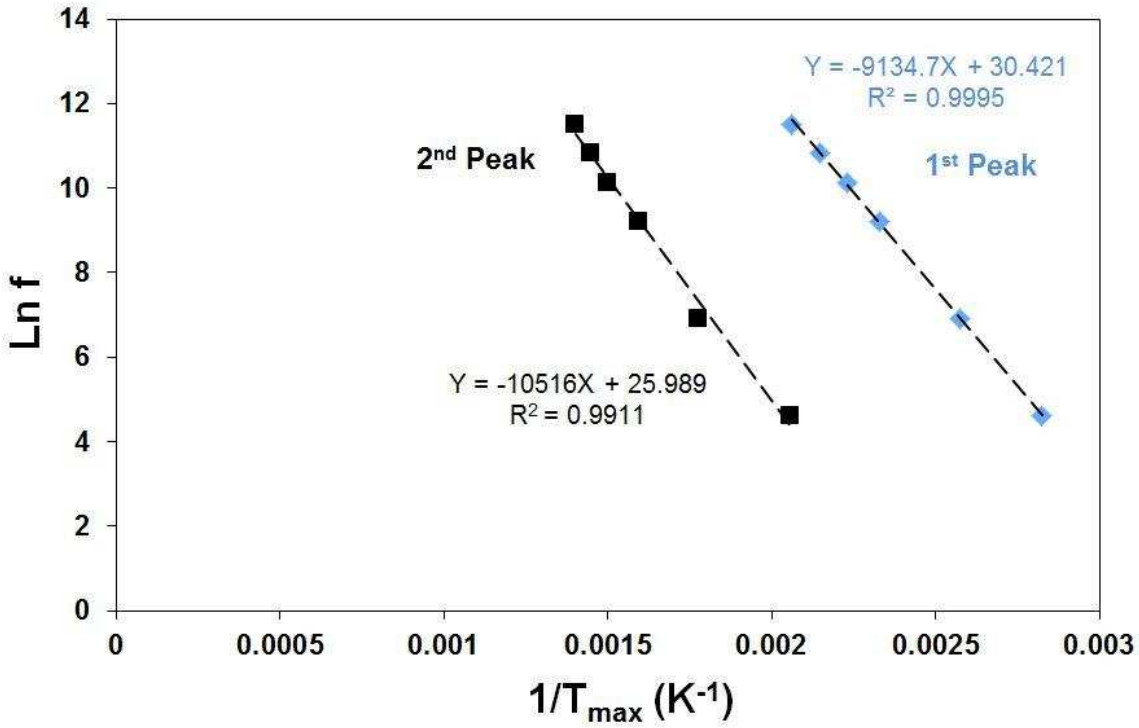

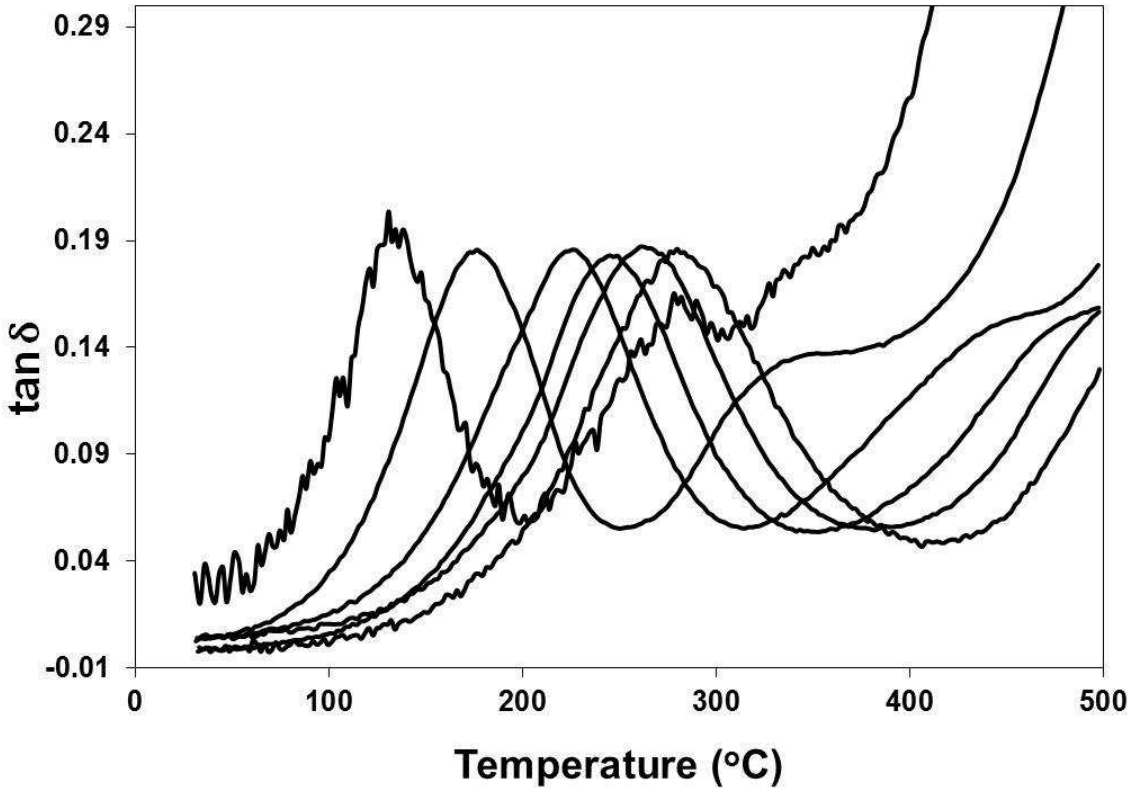

Figure 3. The tan plotted as a function of temperature for the glass ICIE2.

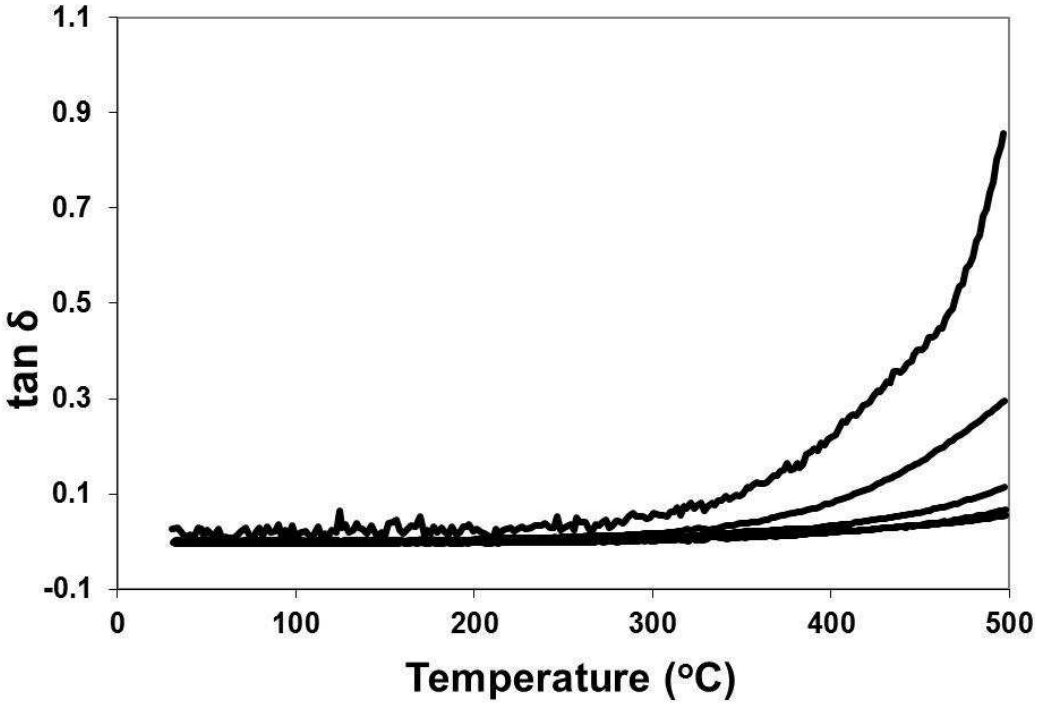

Figure 4. The tan plotted as a function of temperature for the lowest soda content glass ICIE4.

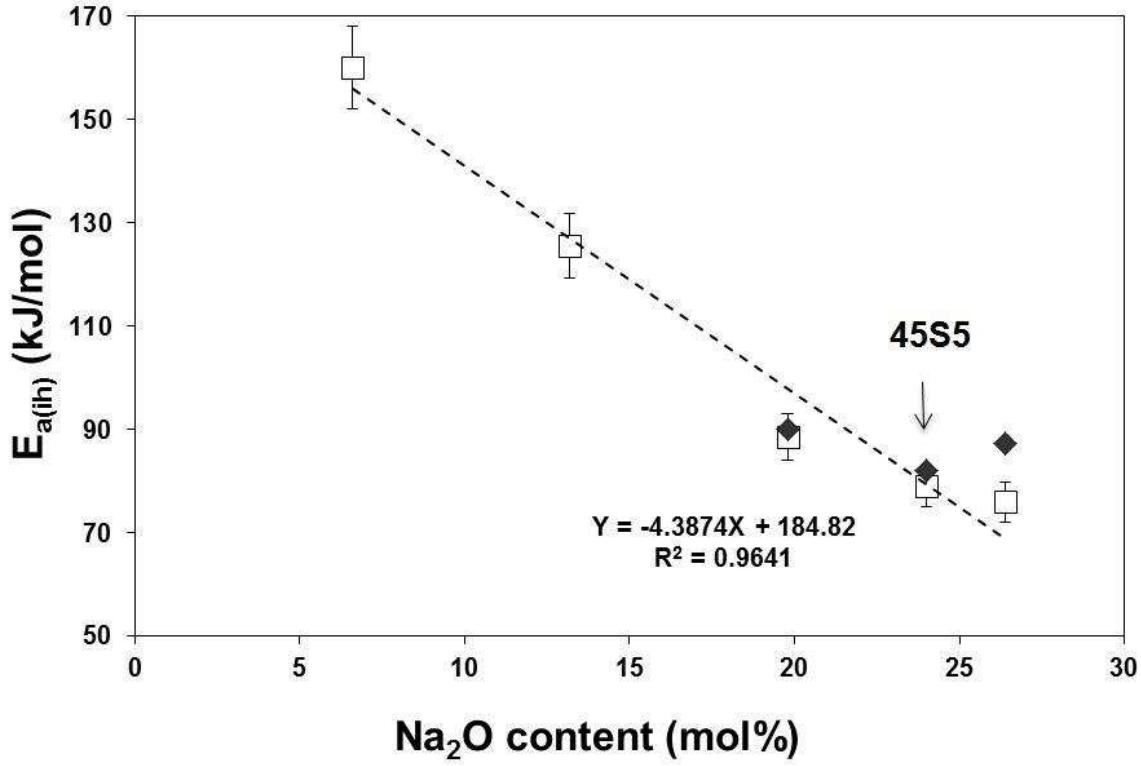

Figure 5. Activation Energy Plotted against Na2O content for the A series glasses and the 45S5 composition. (□ = Relaxation 1 and ♦ = Relaxation 2)

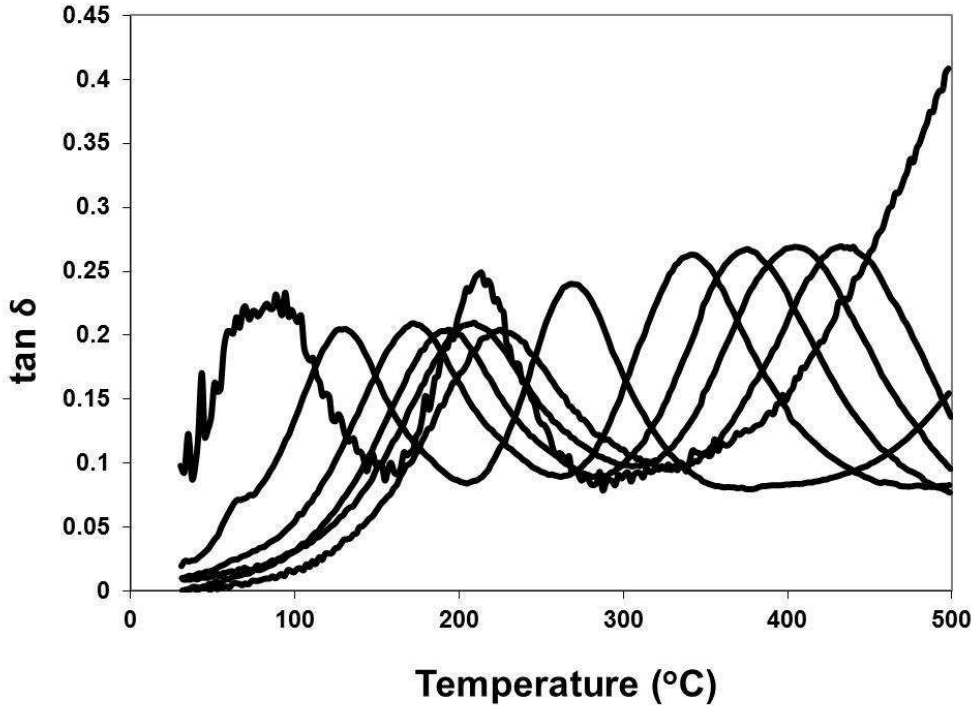

Figure 6. The tan plotted against temperature for 45S5 glass.

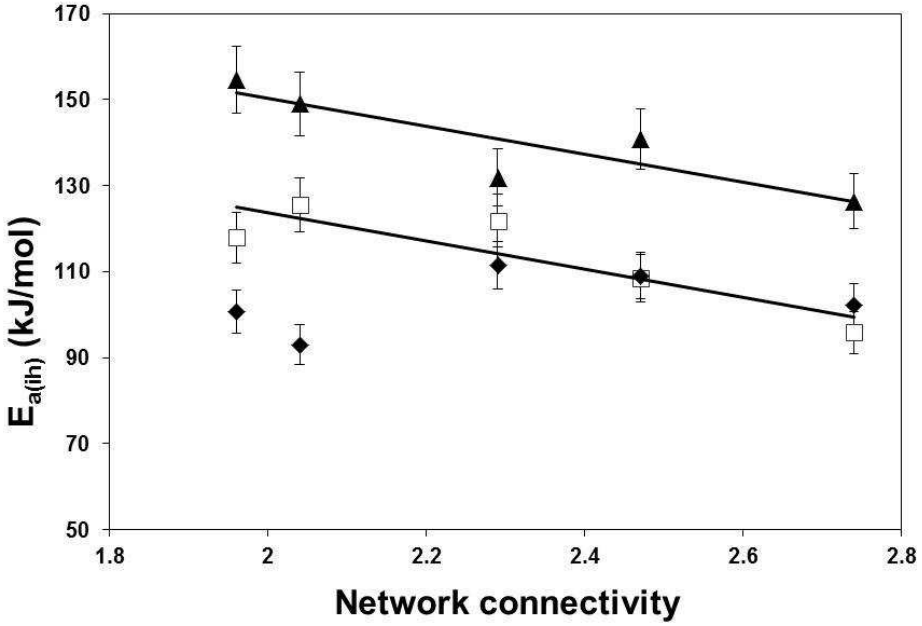

Figure 7. Activation energies for ion hopping plotted against NC, 5% error was applied. (▲= mixed alkali glasses; □= Na containing glasses; ♦= K containing glasses)

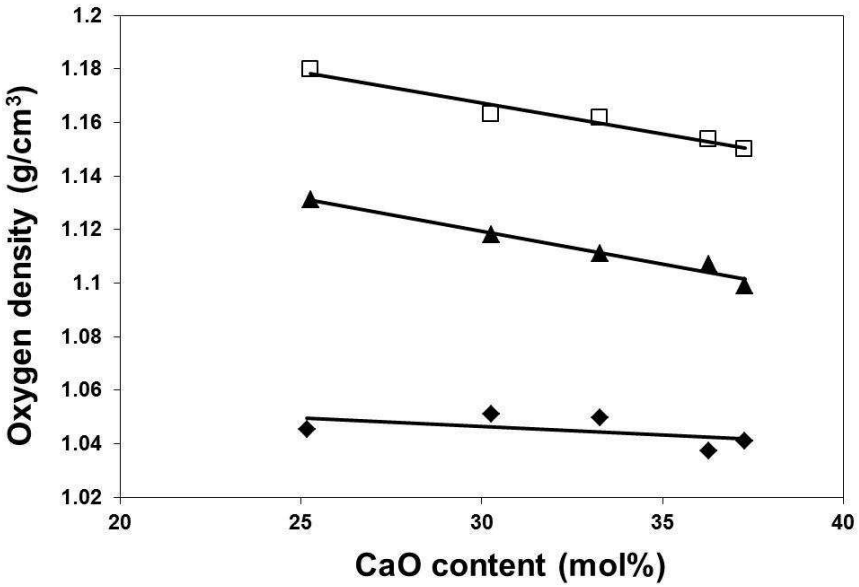

Figure 8. The influence of CaO content on the glass oxygen density. (▲= mixed alkali glasses; □= Na containing glasses; ♦= K containing glasses)

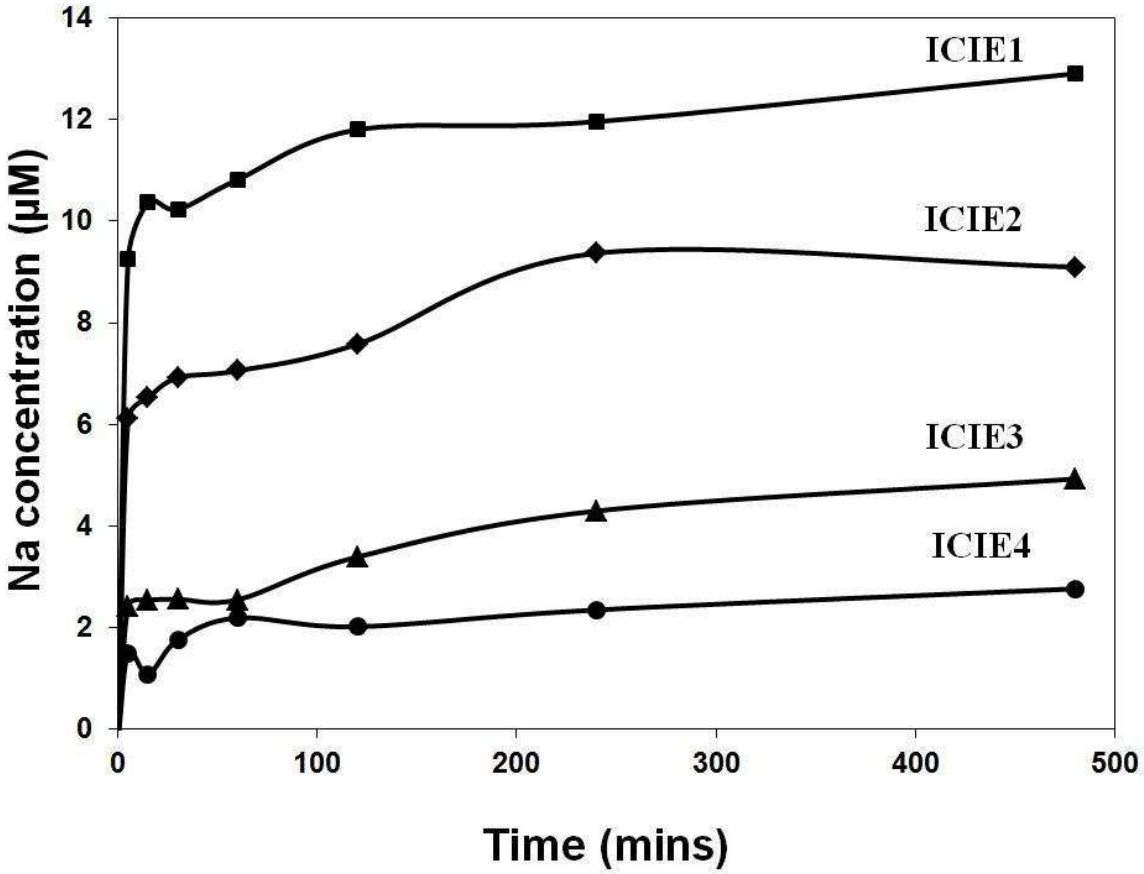

Figure 9. Sodium release as a function of time for the A series glasses. Y units corrected for relative molecular mass and normalized to Na content of glass.

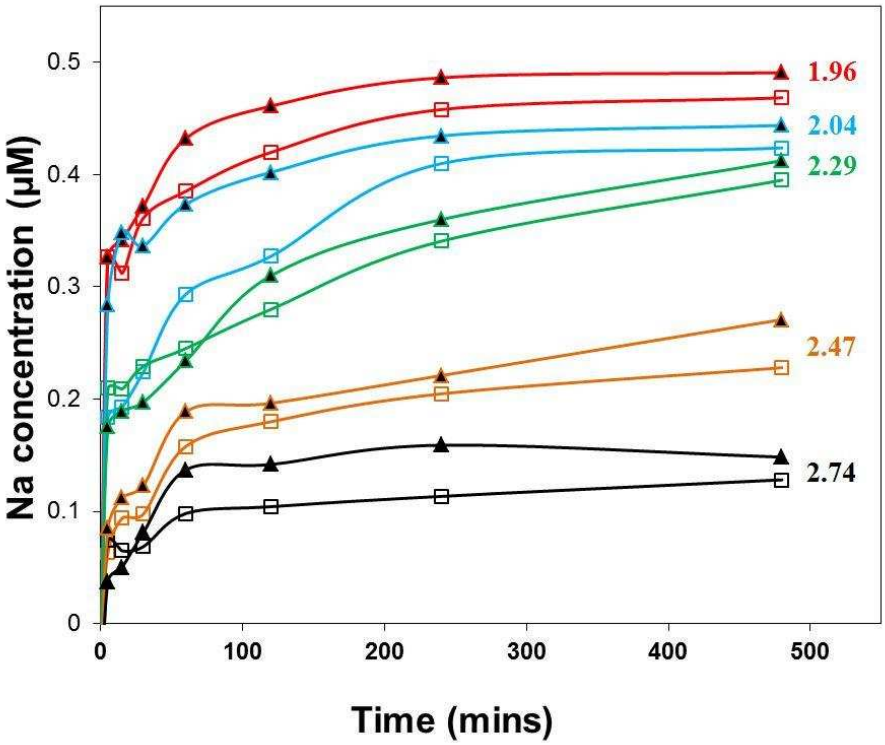

Figure 10. Sodium release as a function of time for series B and D glasses. (▲= mixed alkali glasses and □= Na containing glasses)

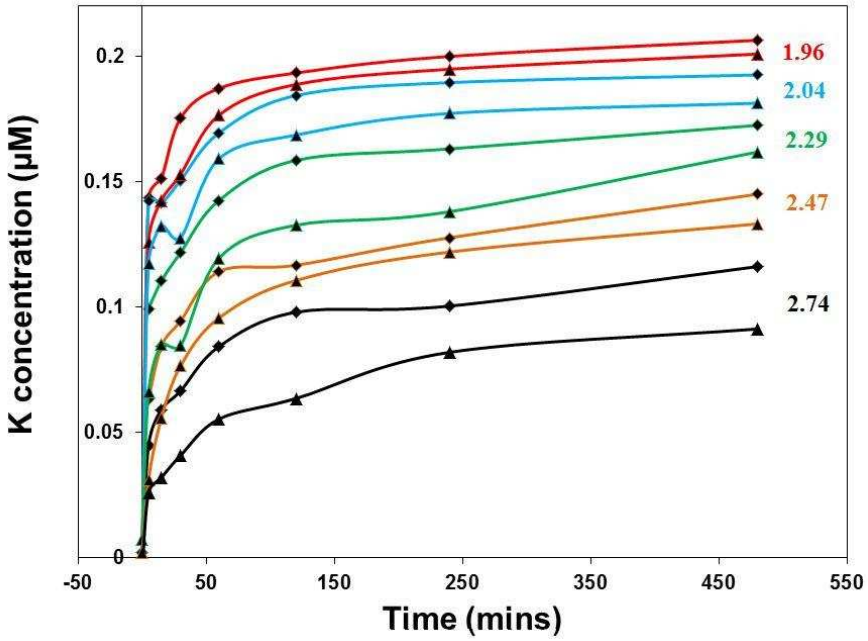

Figure 11. Potassium release as a function of time for series C and D glasses. (▲= mixed alkali glasses and ♦= K containing glasses)

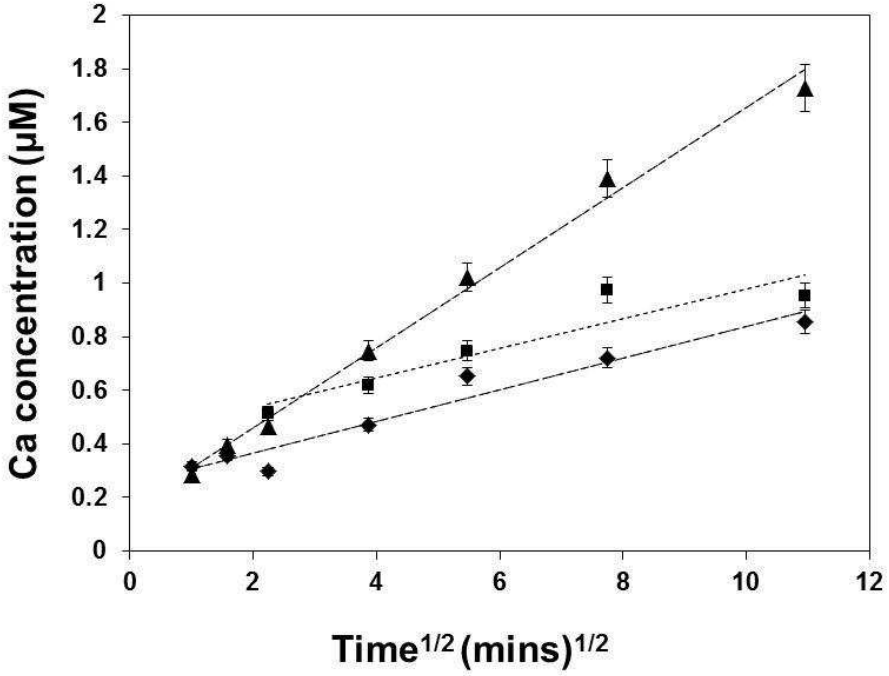

Figure 12. Calcium release for the ICIE9 glass plotted against the square root of time at □=20 oC; □=37 oC and □=50oC.

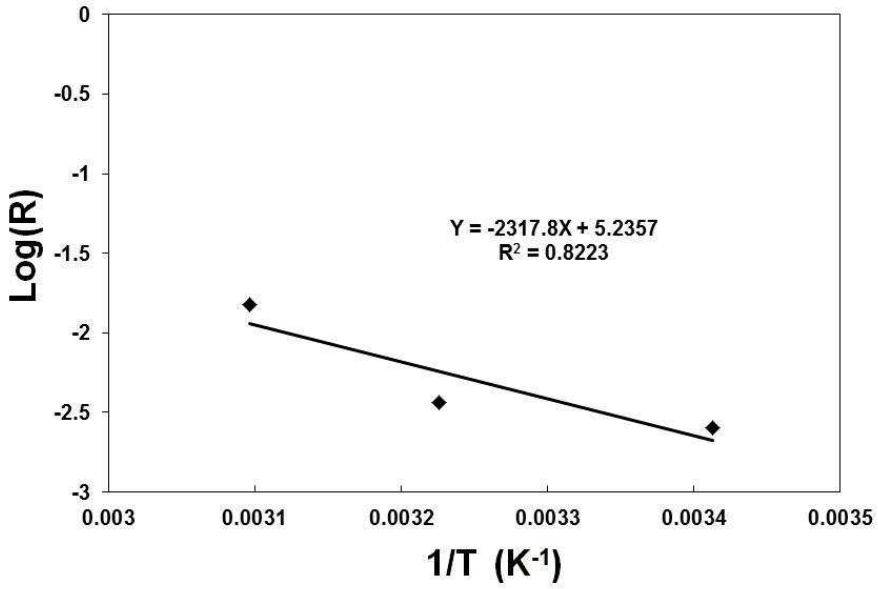

Figure 13. The log of the rate of dissolution against reciprocal temperature of ICIE9 for Ca release.